Journal of Fiber Bioengineering and Informatics 16:4 (2023) 341–350

Cite as: J. Tu et al.
doi:10.3993/jfbim02181

Compatibility of Sleeve Fabric of Tight Alpine Ski Suit with Skin Deformation

Jing-Wen Tu, Yi-Jia Yan, An-Hua Zhong*

Wuhan Textile University, No. 1 Fangzhi Road, Hongshan District, Wuhan, Hubei 430073, China

Abstract

This paper uses a combination of alginate impression and body surface tracing to study the skin deformation mechanism of upper limbs in alpine skiing, and the sleeve pieces were divided into 5 regions combined with the characteristics of human heat and sweat. The thickness, permeability and constant elongation of 7 kinds of elastic fabrics commonly used in tight sports clothing were tested to provide a quantitative basis for fabric compatibility in different zones. The results showed that the skin deformation in the elbow joint area was significant, the transverse changes were mostly stretching, and the longitudinal changes were mostly contraction; the characteristics of heat and sweat in upper limbs were distinct, which could be divided into shoulders, upper arms and below the elbow joint; the order of fabric permeability is as follows: $6 > 3 > 7 > 4 > 1 > 2 > 5$, the order of warp tensile elastic modulus is as follows: $7 > 6 > 1 > 5 > 2 > 4$, the order of weft tensile elastic modulus is as follows: $1 > 3 > 7 > 6 > 5 > 2 > 4$; the abc zones of the sleeve are dominated by the demand for air permeability, which is compatible with 3#, 7# and 6# fabrics respectively, the de zones are dominated by the demand for tensile elasticity, which is compatible with 4# and 2# fabrics respectively.

Keywords: Skin deformation; Tight clothing; Elastic fabric; Structure partition; Alpine skiing

1 Introduction

As the third motion feature of the human body, the skin expands and contracts during motion of different degrees, which can be used to guide the structural design and fabric selection of tight-fitting clothing [1]. Many scholars have conducted relevant research on skin deformation in recent years. Feng [2] measured skin stretch in dynamic and static postures through a 3D scanning system and discussed the convenience of protective clothing; Zhang [3] established a regression model of the lower limb joint movement angle and skin deformation rate to provide a basis for the design of longitudinal slack in pants; Luo [4] studied lower limb skin deformation, skeletal muscle activity and fabric properties to optimise the design of tight-fitting cycling shorts. In this paper, alginate impression combined with body surface tracing is used to obtain the upper limb

*Corresponding author.
Email address: zhongah@yeah.net,291027960@qq.com (An-Hua Zhong).

1940–8676 / Copyright © 2023 Textile Bioengineering and Informatics Society
Dec. 2023

skin deformation data during alpine skiing, and the sleeve structure is divided according to the characteristics of heat and sweat of the human body. Then, 7 kinds of elastic fabrics commonly used in tight sports clothing are selected for thickness, permeability and constant elongation tests to provide a quantitative basis for the compatibility of fabrics in different zones so that the sleeve fabric can better meet the needs of upper limb movement.

2 Methods

2.1 Skin Deformation Experiment

In this experiment, five young females aged 23 to 25 years, with a height of 162 cm to 165 cm and a weight of 50 kg to 60 kg, were selected as experimental subjects. Alginate was used as the experimental material, and the skin deformation experiment was carried out with body surface tracing. According to the reference points and baseline of the key parts of the human upper limb, the experimental measurement line segment was drawn, and the arm impression was carried out by selecting four basic movements in alpine skiing: sliding, downhill, rotary extension and rotary lift, as shown in Fig. 1 and Fig. 2.

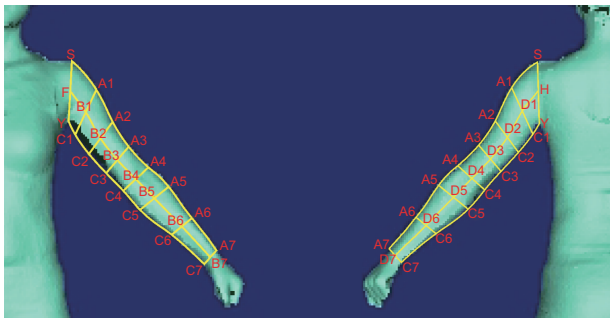


Fig. 1: Measuring line



(1) Natural sagging (2) Sliding (3) Downhill (4) Rotary arm extension (5) Rotary arm lifting

Fig. 2: Experimental actions

2.2 Fabric Testing

2.2.1 Basic Parameter Test

Seven kinds of high-elastic fabrics commonly used in tight-fitting sportswear are selected for testing. Balance, fabric thickness tester and permeability tester are used for testing, and the

sample size is 20 cm×20 cm.

2.2.2 Constant Elongation Test

With reference to "GB/T 3923.1-2013 Textile Fabric Tensile Properties", the tensile forces of 7 kinds of fabrics are tested at the tensile rates of 20%, 40%, 60%, 80% and 100% [5], respectively. The sample size is 5 cm×15 cm.

3 Results and Discussion

3.1 Skin Deformation Analysis and Sleeve Structure Partition

3.1.1 Skin Deformation Characteristics of Upper Limbs

Due to the subjects' body size variation, the Cronbach α coefficient [6] was used for reliability analysis first, and the results (0.942) indicated a high quality of reliability of the experimental data.

The average of the measurement data from 5 subjects was taken for the next analysis. The formula is as follows:

$$k = \frac{b-a}{a} \times 100\% \tag{1}$$

In the formula, 'a' is the length of line segment when the arm drops naturally; 'b' is the length of line segment under each action; 'k' is the rate of skin deformation, $k < 0$ means skin contraction, $k > 0$ means skin stretching.

The overall skin deformation rate in the longitudinal and transverse directions of the upper extremities are shown in Fig. 3. The four longitudinal lines are all in a state of contraction, SA7 (longitudinal line of arm length) and FB7 (longitudinal line of front side) deform relatively significantly in the process of movement change, and the maximum deformation rate occurs during downhill. In contrast, the deformation rate of YC7 (axillary longitudinal line) and HD7 (posterior longitudinal line) is relatively stable. Except for A4-B4-C4-D4-A4 (elbow circumference), the other seven transverse lines are contracted due to the elbow's large bending angle during downhill, which causes the skin to stretch. The changes of S-F-Y-H-S (arm root circumference), A1-B1-C1-D1-A1 (upper arm circumference) and A6-B6-C6-D6-A6 (1/2 line of wrist circumference and forearm circumference) were generally consistent. Still, the deformation rate of arm root circumference is larger. The variation trend from A2-B2-C2-D2-A2 (1/3 line of upper arm circumference and elbow circumference) to A5-B5-C5-D5-A5 (forearm circumference) was generally consistent, and the deformation was relatively significant. The variation trend of A7-B7-C7-D7-A7 (wrist circumference line) differed from that of the other seven horizontal lines. The maximum deformation of A7-B7-C7-D7-A7 (wrist circumference line) was generated during the downhill action (the maximum deformation rate of the other seven horizontal lines was generated during the sliding action). The deformation rate was greater than that of the other horizontal lines during the process, which was due to the large skin deformation caused by the wrist controlling the direction of the ski pole.

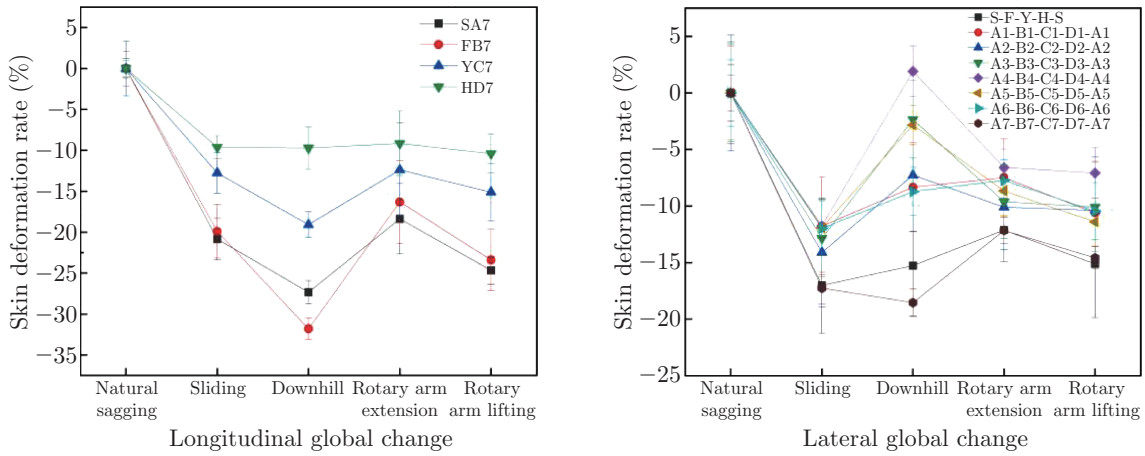


Fig. 3: Overall skin deformation rate

The longitudinal skin deformation rate is shown in Fig. 4. Generally, the variation trend of S-A7 and F-B7 is relatively consistent, and the change amplitude is greater than that of Y-C7 and H-D7. The maximum change rate of each line segment on S-A7 and F-B7 reach −52.63% and −59.34%, respectively. The skin contraction of A3A4, A4A5, B3B4 and B4B5 (elbow fossa) is significant

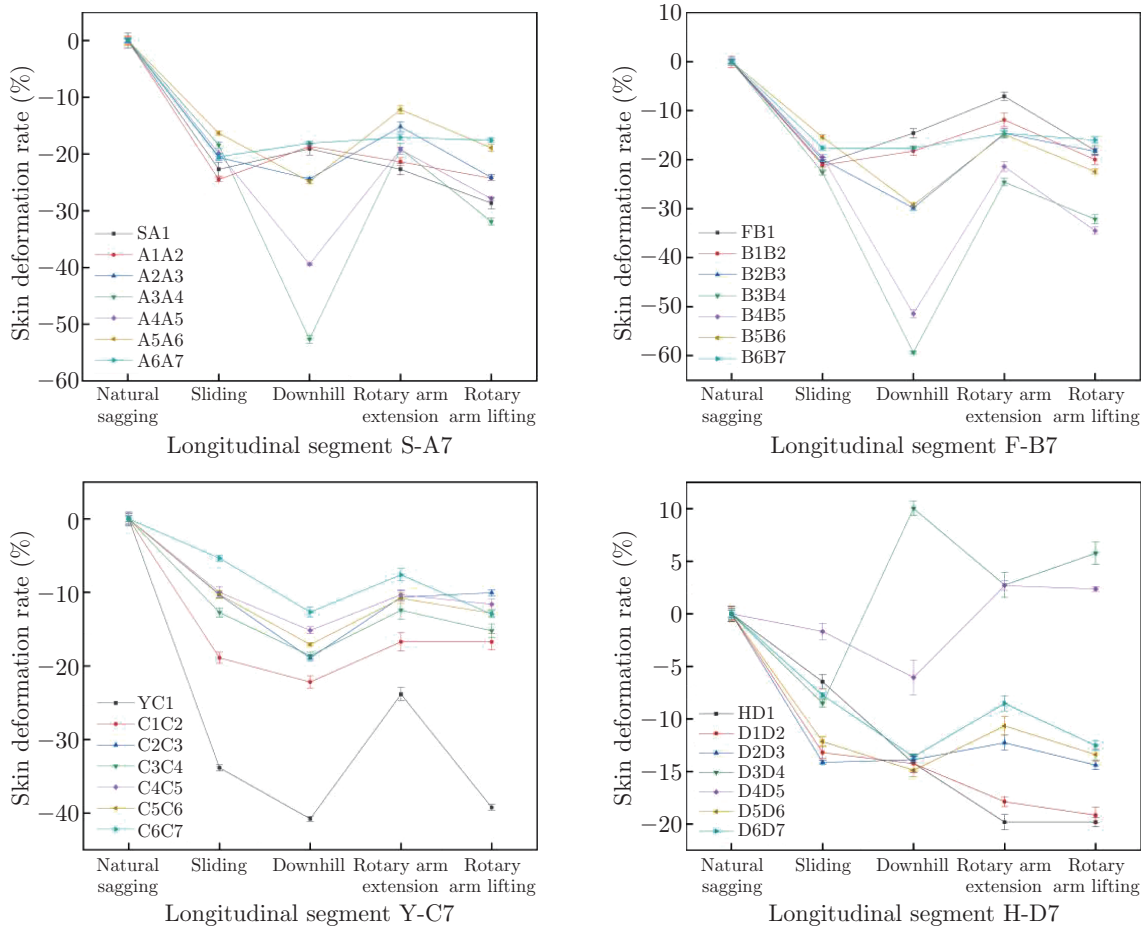


Fig. 4: Longitudinal segmental skin deformation rate

during downhill, and the change of other parts is obvious compared with the initial movement. Still, the deformation is gentle during the movement. The deformation of YC1 measured under the armpit significantly differs from that of other parts, and the maximum deformation rate reaches −40.77% during the downhill motion. This can be explained by the simultaneous contraction of the pectoralis major, biceps and shoulder deltoid muscles during the movement, clamping the upper arm as close to the body as possible to reduce wind resistance. The deformation of each line segment on H-D7 is different, and the deformation rate of HD1 has a large range of about 13%.

Due to the large movement of the elbow joint during the slide down and rotation movements, D3D4 (the upper end of the elbow joint) produces skin stretching and a large deformation. The muscles in D4D5, D5D6 and D6D7 are less developed, and the deformation amplitude is relatively small during exercise.

The transverse skin deformation rate is shown in Fig. 5. Overall, the skin deformation rate is greater on the anterior than the posterior side of the arm, with more significant differences in deformation between the sites.

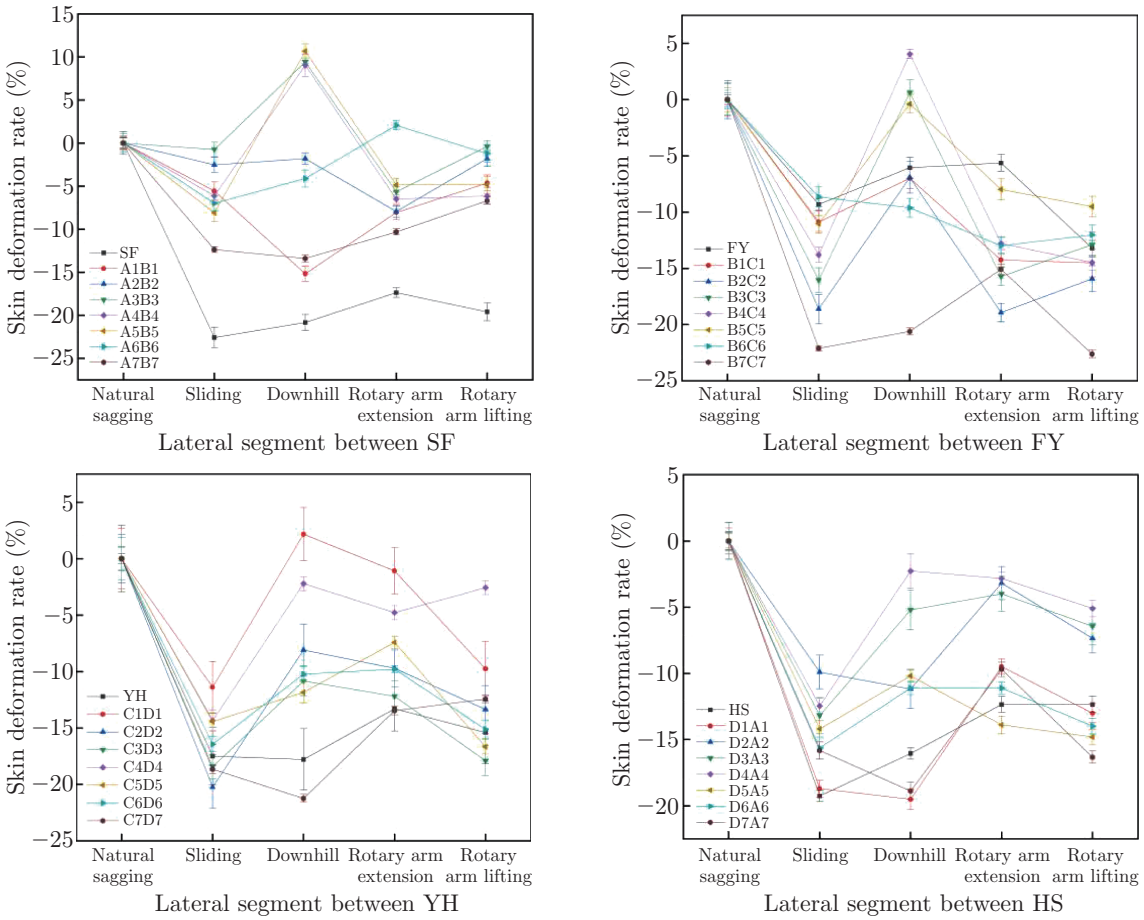


Fig. 5: Transverse segmental skin deformation rate

SF and A1B1 produce the maximum shrinkage deformation during sliding and downhill, respectively. The overall deformation amplitude of A2B2 is relatively gentle. A3B3, A4B4, and A5B5 are located in the cubital fossa, and the deformation trend is generally the same, and the skin stretches downhill. A6B6 slightly stretches the skin when the arm is rotated. The deformation

amplitude of A7B7 is small during the movement, but the deformation rate is large compared with the initial movement. The skin deformations of FY and B1C1 are gentle in the movement process, and the deformation rates of both reach the maximum when the arm is raised in rotation. The deformation trends of B2C2, B3C3, B4C4 and B5C5 were roughly the same, and the deformation rates reached the maximum during sliding and the minimum during the downhill movement. Among them, B3C3 and B4C4 stretch the skin during the downhill movement. B6C6 deformation amplitude is flatter. B7C7 changes significantly, and the maximum deformation rate reaches -22.61%. The deformation rate of YH is larger than that of the initial movement, and the deformation amplitude is relatively gentle during the process. C1D1 produces skin stretching during the downhill movement. C2D2 and C3D3 have the same deformation trend. C4D4 has the largest deformation when sliding, and the deformation in the rest of the movement is relatively small and flat. The deformation trend of C5D5 and C6D6 is the same, and the deformation rate is large. C7D7 produces the largest deformation when the subject is sliding and going downhill. The deformation trends of D3A3 and D4A4 are generally consistent, with the largest deformation rate during sliding, and the deformation rates of other actions are relatively small. The deformation rates of HS and D1A1 when the subject is sliding and going downhill are relatively large, reaching $16\% \sim -20\%$. Under the influence of triceps force, D2A2 has the highest deformation rate during the downhill movement. The deformation trend of D5A5 and D6A6 is generally the same with gentle deformation amplitude. The deformation amplitude of D7A7 changes significantly, and the maximum deformation rate occurs during the downhill motion.

3.1.2 Characteristics of Heat and Humidity Sweating

In the body-costume-environment system, the human body must maintain a constant temperature, and the function of clothing is to ensure that the heat and humidity conditions of the human body are within the range of human physiological regulation under various climatic and physiological conditions. Smith Caroline J [7] et al. studied the changes in sweat volume of the female human body under different exercise intensities, which can be used as the theoretical basis for the division of the hot, wet sweating area of the female upper limb. As shown in Fig. 6, the characteristics of hot and wet sweating in the upper limbs are obviously distinguished, with the largest sweating rate in the lower arm and elbow joint area, followed by the shoulder and smallest sweating rates in the upper arm.

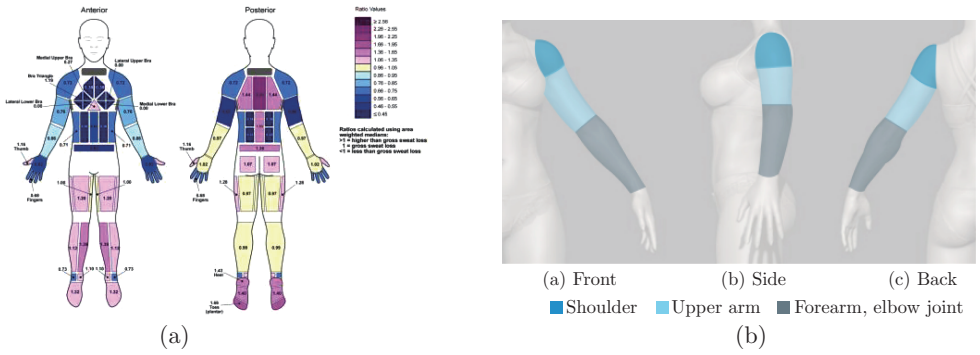
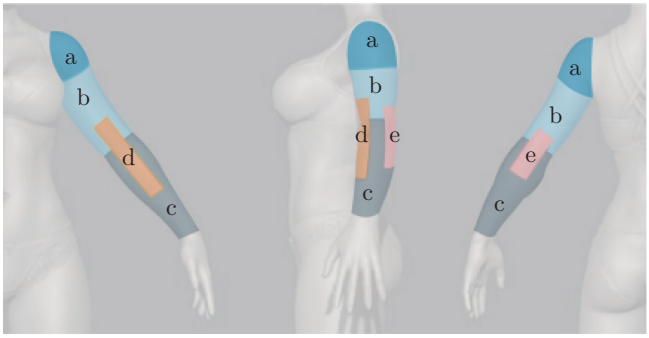


Fig. 6: (a) Sweating characteristics of female body; (b) Upper limb sweating division

3.1.3 Sleeve Structure Partition

Considering the skin deformation and the characteristics of heat, humidity and sweat, and combining with the principle of minimum segmentation, the sleeve is designed in sections, as shown in Fig. 7. Except for the elbow fossa and the convex side, the skin deformation characteristics of area 1, 2, and 3 are roughly the same, so they are mainly divided according to the characteristics of heat, humidity and sweating. The elbow joint area has a high activity intensity, so the skin deformation is given priority, and it is divided into zone 4 and zone 5.



(a) Front (b) Side (c) Back

Fig. 7: Sleeve structure partition

3.2 Fabric Performance Analysis and Compatibility Research

3.2.1 Basic Parameter

The test results of gram weight, thickness and air permeability of the fabric are shown in Table 1. The air permeability of 7 fabrics is ordered from largest to smallest as follows: $6 > 3 > 7 > 4 > 1 > 2 > 5$.

Table 1: Basic parameters of fabric

Number	Fabric composition (%)	Gram weight (g/m^2)	Thickness (mm)	Permeability (mm/s)
1#	PA:SP=75:25	220	0.580	393.970
2#	PA:SP=78:22	250	0.789	389.473
3#	PA:SP=67:33	300	0.620	401.213
4#	PA:SP=74:26	310	0.962	395.276
5#	PA:SP=79:21	200	0.643	325.866
	Average value	256	0.719	381.160
	Standard deviation	43.174	0.141	27.900
6#	T: SP=85:15	180	0.575	463.483
7#	T: SP=84:16	190	0.530	397.783
	Average value	185	0.553	430.633
	Standard deviation	5	0.023	32.850

3.2.2 Fabric Elasticity Analysis

The tensile force results of seven kinds of fabrics in warp and wetted directions are shown in Fig. 8 when the tensile rate is 20%, 40%, 60%, 80% and 100%, respectively.

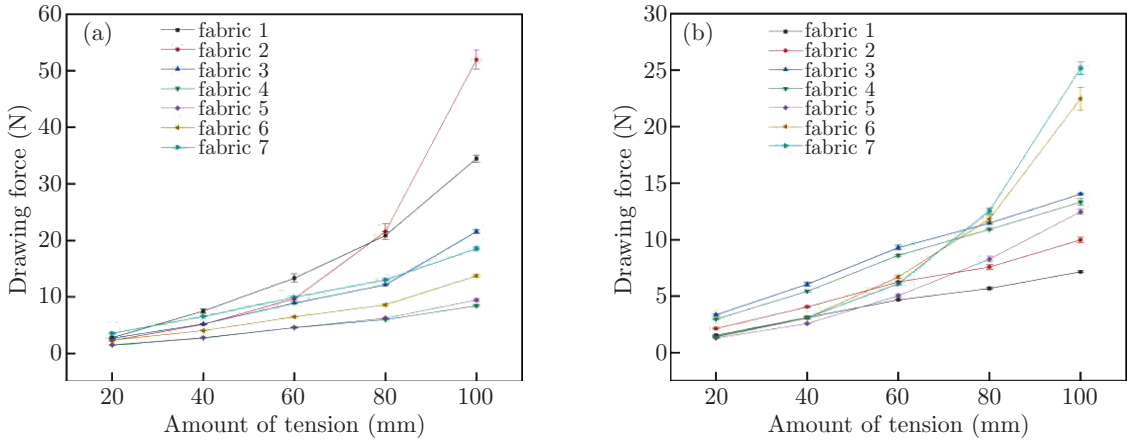


Fig. 8: (a) Relationship between meridional stretch and tensile force; (b) Relationship between zonal stretch and tensile force

The mathematical regression models of tensile force and elongation of 7 kinds of fabrics are obtained by linear fitting the experimental data of constant elongation. The goodness of fit R^2 of the models is greater than 0.8, indicating that the models have good linear correlation.

Table 2: Regression model of tensile force-elongation

Number	Regression model (Warp direction)	R^2	Regression model (Zonal direction)	R^2
1#	$y = 0.38x - 7.21$	0.951	$y = 0.07x + 0.30$	0.995
2#	$y = 0.58x - 16.6$	0.814	$y = 0.10x + 0.24$	0.995
3#	$y = 0.22x - 3.3$	0.925	$y = 0.13x + 0.81$	0.996
4#	$y = 0.09x - 0.54$	0.988	$y = 0.13x + 0.40$	0.997
5#	$y = 0.10x - 0.86$	0.970	$y = 0.14x - 2.48$	0.962
6#	$y = 0.14x - 1.13$	0.951	$y = 0.25x - 6.19$	0.901
7#	$y = 0.18x - 0.57$	0.984	$y = 0.28x - 7.39$	0.870

Tensile elastic modulus is one of the indicators to measure the difficulty of elastic deformation of fabric, which can provide a quantitative basis for fabric selection in different sections of sleeve pieces. The calculation formula [8-9] is as follows:

$$E = \frac{\sigma}{\varepsilon} = \frac{F/A}{k \times 100\%} \tag{2}$$

In the formula, E is the tensile elastic modulus, N/mm^2; σ is stress, N/mm^2; ε is the deformation rate, %; F is the tensile force required when the specimen is stretched to twice the original length [8], N; A is the section area, that is, the product of sample thickness and sample width, mm^2; k is the fitting coefficient. The tensile elastic modulus of 7 fabrics is shown in Table 3.

Table 3: Elastic modulus of fabric

Number	1#	2#	3#	4#	5#	6#	7#
Meridional elastic modulus (N/mm^2)	3.13	2.27	3.16	1.95	2.94	3.41	3.89
Zonal elastic modulus (N/mm^2)	3.53	2.53	3.48	2.13	2.77	3.13	3.39

In summary, the order of the meridional tensile elastic modulus of the seven fabrics is $7 > 6 > 3 > 1 > 5 > 2 > 4$. The order of the zonal tensile elastic modulus is $1 > 3 > 7 > 6 > 5 > 2 > 4$. In contrast, the elastic modulus of fabric No. 4, 2 and 5 is small in warp and weft direction. No. 1, 2, 3, and 4 fabrics have less warp elastic modulus than the weft, and No. 5, 6, and 7 fabrics have more warp elastic modulus than the weft.

3.2.3 Fabric Compatibility Design

Based on the above analysis data, the permeability requirements of each section of the sleeve piece are as follows: c>a>b. Therefore, 3# fabric is selected for zone a, 7# fabric is selected for zone b, and 6# fabric is selected for zone c. The skin deformation in zone d is transverse stretching, and the fabric with a small zonal modulus and good air permeability should be matched. 4# fabric should be selected. The overall skin deformation in zone e is longitudinal stretching. It is necessary to match fabrics with small meridian modulus and choose 2# fabrics. The result is shown in Fig. 9.

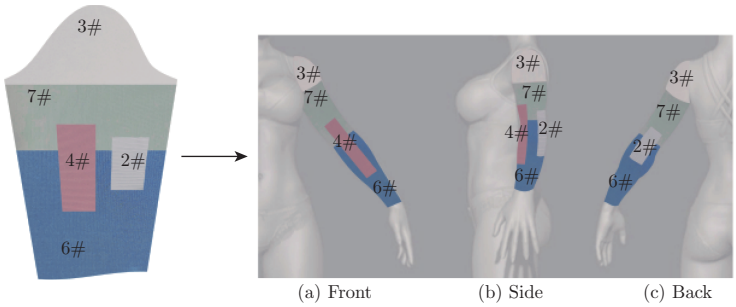


Fig. 9: Fabric compatibility design

4 Conclusion

Alginate impression combined with body surface tracing was used to study the upper limb skin deformation in typical actions of alpine skiing. Combined with the characteristics of human heat and humidity sweating, the sleeve structure is divided so that the sleeve fabric can better meet the needs of upper limb movement. Seven kinds of high-elastic fabrics commonly used in tight-fitting sports clothing are selected for thickness, air permeability and fixed elongation tests, providing a quantitative basis for the compatibility of fabrics in different zones, and the following conclusions are drawn:

(1) The skin deformation characteristics of different parts of the upper limb during exercise are different. Longitudinally, the skin contraction changes are very significant, with the maximum

skin shrinkage rate reaching −59% in the elbow fossa region, the skin contraction of the shoulder joint and armpit is more obvious. The skin stretching occurs only in the outer convex side of the elbow joint, and the stretching rate is 10%. Laterally, skin stretching occurs in the elbow fossa area, with a maximum stretching rate of 11%, and skin contraction occurs in other parts. On the whole, the deformation of the elbow joint area is significant; the transverse change is mostly tensile, and the longitudinal change is mostly contraction.

(2) According to the characteristics of skin deformation and heat, humidity and sweat, the sleeve is divided into five regions: 'abcde', 'ABC' region is mainly based on air permeability demand, and 'de' region is mainly based on tensile elasticity demand.

(3) To match the sleeve segment with the most suitable fabric for air permeability and warp and weft elastic modulus, 7 commonly used high elastic fabrics are selected for testing. The order of fabric permeability is: $6 > 3 > 7 > 4 > 1 > 2 > 5$; The order of the elastic modulus of warp tensile is as follows: $7 > 6 > 3 > 1 > 5 > 2 > 4$; The order of the zonal tensile elastic modulus is $1 > 3 > 7 > 6 > 5 > 2 > 4$.

(4) According to the air permeability and stretch elasticity requirements of the sleeve segment, zone 'a' is matched with 3# fabric, zone 'b' is matched with 7# fabric, zone 'c' is matched with 6# fabric, zone 'd' is matched with 4# fabric, and zone 'e' is matched with 2# fabric.

References

[1] Armstrong H J, Pearson, Patternmaking for fashion design: Pearson new international edition. New Havenpearson Higher Education. 2015.

[2] Ming Ming Feng, Li Liu, Hui Zou, Xiao Hui Zheng, Xiao Chen Li. Research on ease of protective clothing based on three-dimensional human body scanning [J]. Journal of Fiber Bioengineering & Informatics, 2019, 12(2).

[3] Zhang F S, Wang Y Z, Study on skin deformation based on angle change of lower limb joint activity in young women. Journal of Beijing Institute of Fashion Technology (Natural Science Edition). 2022, 42(03): 35-43. DOI:10.16454/j.cnki.issn.1001-0564.2022.03.007.

[4] Luo S H, Structural partition design of functional tight cycling shorts. Knitting Industries. 2020(10): 66-70.

[5] Wu J H, Yu W D, The elasticity and clothing pressure of knitted fabrics [J]. Journal of Wuhan University of Science and Engineering, 2006(01): 21-25.

[6] Eisinga Rob, Grotenhuis Manfred te, Pelzer Ben, The reliability of a two-item scale: Pearson, Cronbach, or Spearman-Brown. International Journal of Public Health 2013, 58(4).

[7] Smith Caroline J, Havenith George. Body mapping of sweating patterns in athletes: a sex comparison [J]. Medicine and science in sports and exercise, 2012, 44(12).

[8] Yu W D, Textile Physics [M]. Donghua University Press, 2002.

[9] Ai Y R, Research on the Pressure of Seamless Tights Running Pants Based on Muscle Division [D]. Shanghai University of Engineering Science, 2021. DOI:10.27715/d.cnki.gshgj.2021.001035.